Combined Operation of Photovoltaic and Biogas Plants for Optimal Transformer Loading

Katharina Bär[a,*], Abdessamad Saidi[a], Christoph Hackl[b], Wilfried Zörner[a]

[a]Technische Hochschule Ingolstadt, Institute of New Energy Systems, Esplanade 10, 85049 Ingolstadt, Germany
[b]Munich University of Applied Sciences, Department for Electrical Engineering and Information Technology, Lothstraße 64
80335 Munich, Germany
katharina.baer@thi.de

Due to the ability to produce electricity on demand, biogas plants show a high potential to avoid grid overload caused by short-term feed-in fluctuations of photovoltaic (PV) power plants at the distribution level of the electricity grid. To optimise the balancing approach, the present research is focused on the development of a control system for a privately operated, agricultural biogas plant considering high feed-in gradients of surrounding PV power plants. A ground-mounted PV power plant is modelled using Matlab®/ Simulink™ to forecast the PV power feed-in in high resolution. Among various modelling approaches the five-parameter single diode R_p-model is selected as the central model for a PV cell. To analyse the behaviour of the DC-output of a PV array considering shading effects caused by cloud drift the model is modified from a module to an array system. The computed DC-output of the PV plant is compared in terms of accuracy to the rated value of manufacturer data and analysed in terms of computation time to be integrated within a short time horizon as input data in the control system.

1. Introduction

The rising costs of fossil fuels and growing need to reduce greenhouse gas (GHG) emissions increase the importance of renewable energy technologies (Valencia et al., 2018). Shortly, the installed power generation capacities of renewable energies will by far exceed the conventional energy production. Already in 2017, 216 TWh (36 % of the gross electricity consumption in Germany) was produced from renewable energy sources (Bundesministerium für Wirtschaft und Energie (BMWi), 2018). By 2030, the ratio of fossil fuel- and renewable-based electricity production is expected to be inverted (Heinrich Böll Foundation, 2018). The provided power of wind and solar energy are, however, continuously changing due to local environmental variations such as solar irradiance, wind strength and temperature. Due to the rising amount of variable renewable electricity generators, electricity generation will arise primarily according to availability. To ensure electricity grid stability in future, advanced energy system management is required (Stark et al, 2017). The resulting incongruence between generation and demand will cause periods with a lack or a surplus of electricity in the grid. During underproduction, additional electricity production is required, while during periods of overproduction the surplus electricity has to be stored. Therefore, new solutions in the fields of load management and new storage technologies as well as grid expansion have to be considered (Liu et al., 2018). The electricity generation from biomass plants (Stark et al., 2018), especially from biogas plants is independent of weather conditions, hence, allows a controllable (Häring et al., 2017) and demand-driven energy provision (Dotzauer et al., 2018).

2. Methodology

2.1 Biogas Plant and PV Power Plant at one Grid Connection Point

The focus of the present research is on balancing the intermittent power supply from solar energy with the controllable power generation of a biogas plant at one grid connection point for an optimal transformer loading at the medium voltage distribution grid level, as shown in Figure 1. During time periods of high solar irradiation and a generation of electricity according to EPEX SPOT SE electricity prices of decentral biogas and PV power

plants at the maximum level, the capacity of a grid connection point in the rural medium voltage distribution grid is not sufficient for the overall feed-in (see Figure 1: Initial Situation). With the development of a biogas plant control system with control intervals in a range of seconds (s) short-term, daily occurring grid overload in the rural distribution grid can be avoided which allows an increase of the total energy feed-in of the biogas and PV power plants to the electricity grid (see Figure 1: Optimised Situation).
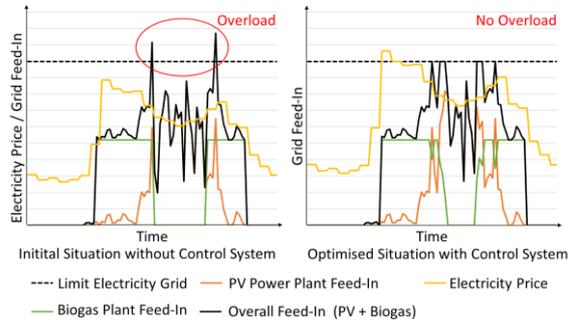
Figure 1: Power Generation of the Biogas Power Plant with a Predictive Control System.

2.2 Demonstration biogas plant

In this context, the privately operated, agricultural biogas plant Zellerfeld in Bavaria, Germany, is used to analyse the behaviour of a system consisting of a biogas plant and a PV power plant (Figure 2).
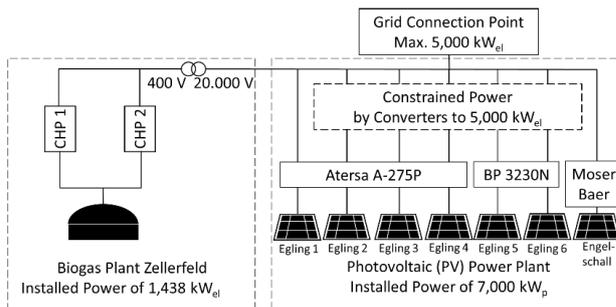
Figure 2: Overview of Biogas and PV Power Plants at Zellerfeld.

The biogas plant has an installed power of 1,438 kW_{el} with two installed combined heat and power (CHP) units (CHP 1: 549 kW_{el}, CHP 2: 889 kW_{el}) resulting in an overall rated power of 700…850 kW_{el}. It shares the grid connection point with seven ground mounted PV power plants consisting of several PV modules connected either in series (N_{ser}) or parallel (N_{par}) with a maximum peak feed-in power of 7,000 $kW_{el,p}$ limited by converters to 5,000 kW_{el} (see Table 1).

Table 1: Number of Modules at PV Power Plant Zellerfeld

	Egling 1	Egling 2	Egling 3	Egling 4	Egling 5	Egling 6	Engelschall
N_{ser}	18	18	18	18	22	22	24
N_{par}	146	146	116	90	107	87	132
Inverter	4	1	2	1	1	1	1
Modules	10,512	2,628	4,176	1,620	2,354	1,914	3,168

Adding the maximum PV power plant feed-in to the total feed-in power of the biogas plant, the peak load at the grid connection point is 6,438 kW_{el}. The circuit breaker, installed at the grid connection point, however, is activated with a reaction time in the range of milliseconds when 5,000 kW_{el} are exceeded. Since an expansion of the grid connection point capacity cannot be realised, it is necessary to take a forecast of the feed-in of the PV system into account for the appropriate scheduling of the biogas plant. To determine the feed-in behaviour of a PV power plant, the power provision of a plant with a 1.5 MW_{el} transformer is analysed. The average feed-in gradient on a sunny day without cloud drift in Bavaria is about 1.6 kW_{el}/s. On a very cloudy and windy day

with fast changing weather conditions, the average feed-in gradient is about 65 kW$_{el}$/s. For the considered maximum PV power feed-in with transformers of an installed power of 7,000 kW$_{el}$ a feed-in gradient of approximately 300 kW$_{el}$/s is obtained (Bär et al., 2018a).

Solar predictions are available with a resolution of 15 min in a range of about 5 km (Sirch et al., 2017). According to the feed-in gradients and spatial size of the considered PV power plant, a prediction with a temporal resolution of a few minutes and spatial resolution of at least 1 km is required for an adequate reaction of the CHP units of the biogas plant. Available cloud data, cloud prediction and the spatial-temporal resolution of the resulting solar radiation prediction have to be increased significantly. To be able to perform a systematic validation of cloud detection and prediction, the radiation and resulting PV feed-in forecast is performed using a measuring system, consisting of cloud cameras and radiation sensors. In addition to the measurement system, standard forecasting methods as well as high-resolution satellite data will be considered.

Besides the feed-in gradient of the PV power plant, a significant system parameter is represented by the dynamic behaviour of the CHP units. A complete switch-off of the CHP units takes approximately about 175 s, which means a switch-off gradient of 3.1 kW$_{el}$/s for CHP 1 unit and 5.1 kW$_{el}$/s for the CHP 2 unit. Operation monitoring as well as feedback from experts revealed that the current state-of-the-art allows for a switch-off gradient of about 10 kW$_{el}$/s. An optimum total switch-off process of the CHP units has a duration of 90 s in the biogas plant Zellerfeld, which is too long to react appropriately to the feed-in gradients of the PV power plant. In order to react adequately to the feed-in performance of a PV system, a time delay of approximately 30 s (feed-in gradient of the PV power plant) has to be considered (Bär et al., 2018b).

2.3 Control system for the combination of a biogas and a PV power plant at one grid connection point

For an efficient control of the power supply within the system, the operation management of the control system has to fulfil several steps to respond to the PV power plant by providing the power from the CHP units of the biogas plants in the correct amount at the expected time t as shown in Figure 3. The overall reaction time T_{ct} is critical, as the control system needs to interface with the grid control point in real time.
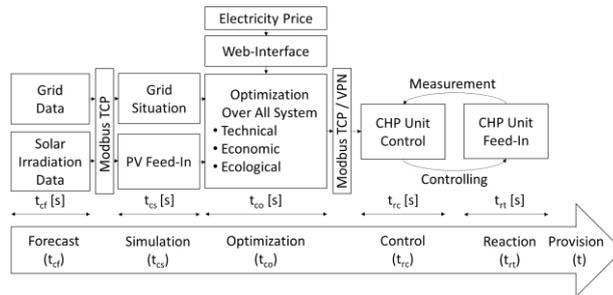
Figure 3: Control System Management Process.

The first step of the control system management process is to forecast the solar irradiation in order to predict the PV array power feed-in (Solar Irradiation Data) and the loads of the electricity grid (Grid Data), which takes the time period t_{cf}.(Figure 3) A Modbus TCP is supplying measurement data of the cloud drift and distribution grid from a monitoring system. These data are used to simulate the electricity grid (Grid Situation) and the PV power plant feed-in (PV Feed-In), which takes the computational time t_{cs}. The core of the project is the development, implementation and verification of a mathematical optimisation algorithm (Optimisation Over All System) to develop CHP unit schedules considering the electricity grid situation (Bär et al., 2018b). The optimisation should lead to a maximisation of the turnover of the biogas plant operator while demand-oriented energy supply within the optimisation time t_{co}. The electricity prices of EPEX SPOT SE (Electricity Price) are taken into account as essential control signals and are read in daily or hourly via a web interface. The timetables created in this way are calculated within the optimisation time t_{co} and, in turn, transmitted via a VPN connection to the CHP unit control (CHP Unit Control), which then regulates the feed-in of the CHPs in the period of time t_{rc}. At the same time, measured data from the CHP (CHP unit Feed-In) and the biogas plant are sent back to the optimisation unit via Modbus TCP. The engine- and generator-caused CHP unit reaction time t_{rt} has to be taken into account as well. The overall reaction time T_{ct} for the control system process can, therefore, be defined as

$$T_{ct} = t_{cf} + t_{cs} + t_{co} + t_{rc} + t_{rt} \tag{1}$$

To forecast the PV power plant feed-in, a model considering partial shading effects, weather and cloud drift forecasts with respect to small-scale spatiotemporal variations at very short forecast horizons has to be

developed. For demand-driven power generation, in this project, even larger array sizes have to be considered in a high resolution of a module in order to take partial shading effects into account. Partial shading is caused by dust, dirt, snowfall, cloud drift, nearby trees or tall structures like buildings or chimneys. This affects the Maximum Power Point Tracking (MPPT) causing efficiency losses of the PV power plant system by reducing the maximum DC-output power of a PV power plant causing multiple peaks in the current-voltage curve ($I - V$ curve). To determine the DC output current of a module, the $I - V$ curve is calculated, applying simulations in Matlab®/Simulink™ (The MathWorks, 2019) according to the ideal single diode model, the single diode R_s-model, the five-parameter single diode R_p-model and the two diode model (Quaschning, 2016) for three different types of cells, which are in operation in the PV power plant in Zellerfeld.

These four established modelling approaches are validated with the datasheets of the manufacturers (see Table 2) and measured data in order to determine the accuracy and computational time.

To model the PV power plant, the following assumptions are considered: (i) The cells are identical and are modelled in ideal condition, i.e. without any electrical losses. (ii) The module temperatures are taken from an installed thermal sensor to consider the effect of local wind speed and ambient temperature.

Table 2: Photovoltaic Modules Data.

	Atersa A-275P	BP 3230N	Moser Baer
Peak power (W)	275	230	230
Number of cells in module N_s	72	60	60
Current at maximum power point I_{mpp} (A)	7.60	7.90	7.80
Voltage at maximum power point V_{mpp} (V)	36.19	29.1	29.50
Short circuit current I_{sc} (A)	8.08	8.40	8.34
Open circuit voltage V_{oc} (V)	45.23	36.7	37.25
Thermal coefficient of I_{sc} (k_i) (%/°C)	0.05	0.105	0.05
Thermal coefficient of V_{oc} (k_v) (%/°C)	-0.35	-0.36	-0.35

3. Results

Comparing the simulation results of the maximum power output in Matlab® Version 2018a (The MathWorks, 2019) with the manufacturers' datasheets, the single diode R_S-model shows the highest accuracy followed by the five-parameter single diode R_p-model, the two diode model and the ideal diode model (see Table 3).

Table 3: Comparison of Computed DC Output to Rated Value of Manufacturer's Data (in W) of PV Modules and Deviation from Data Sheet.

	Atersa A-275P	BP 3230N	Moser Baer
Ideal diode model	296 (+7.7 %)	249 (+8.2 %)	251 (+9.3 %)
Single diode R_s-model	274 (-0.3 %)	229 (-0.6 %)	230 (+0.1 %)
Single diode R_p-model	273 (-0.9 %)	228 (-1.1 %)	229 (-0.3 %)
Two diode model	280 (+1.9 %)	234 (+1.8 %)	236 (+2.5 %)

Table 4: Computation Time (s) in Matlab® for a PV Module.

	Atersa A-275P	BP 3230N	Moser Baer
Ideal diode model	0.19	0.19	0.19
Single diode R_s-model	0.24	0.23	0.24
Single diode R_p-model	0.25 (Simulink™: 8.11)	0.24 (Simulink™: 6.72)	0.24 (Simulink™: 7.44)
Two-diode model	0.26	0.25	0.25
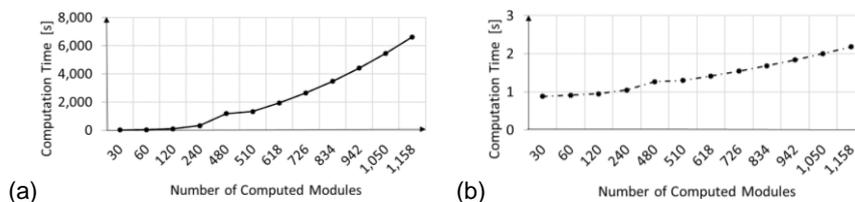
Figure 4: Computation Time in Simulink™ (a) and in Matlab® (b).

Table 4 shows the computation time for the four different modelling approaches in Matlab® and Simulink™. The ideal diode model has the shortest simulation time in Matlab® due to its simple structure and the lowest number of parameters, while the two-diode model has the longest simulation time due to the inclusion of two diodes and the complex iteration to calculate the values for R_s and R_{sh}. By comparing the model accuracy for maximum power of a module and the total computational time, the R_p -model and the R_s-model show similar results (see Table 3 and Table 4). As the R_s -model is not considering the effect of recombination losses of a PV cell, the five-parameter single diode R_p-model is selected for the control system, representing a compromise of accuracy and computation time. According to Table 4, the simulation of the five-parameter R_p-model is almost 40 times faster in Matlab® compared to Simulink™. In the following the five-parameter single diode R_p-model is presented in detail.

To determine the $I - V$ curve of the five-parameter single diode R_p-model, the photovoltaic current I_{ph} as well as the diode current I_D and the shunt current I_{sh} have to be calculated, considering the electron charge q =1.60217646x10−19 C, the Boltzmann constant k=1.3806503x10−23 J/K, the PV cell temperature T, the diode quality factor n, the series resistance R_s, the shunt resistance R_{sh} and the diode saturation current I_0 (Habbati et al., 2014). The current I to a given V in the Interval $m \in [m, m+1]$ can be calculated with the iteration method

$$I(m + 1) = I_{ph} - I_D - I_{sh} = I_{ph} - I_0 \cdot \left(e^{\frac{q \cdot (V + I(m) \cdot R_s)}{n \cdot k \cdot T}} - 1 \right) - \frac{V + I(m) \cdot R_s}{R_{sh}} \qquad (2)$$

The photovoltaic current I_{ph} depends on the solar irradiance G, the cell temperature T, the irradiance G_{STC}, the temperature T_{STC}, the photovoltaic current $I_{ph,STC}$ at standard test condition (STC) and the temperature coefficient for short circuit current K$_i$, i.e.

$$I_{ph} = \frac{G}{G_{STC}} \cdot (I_{ph,STC} + K_i \cdot (T - T_{STC})) \qquad (3)$$

To consider the temperature for the calculation of the diode saturation current I_0, the variation of the temperature coefficient K_v for open circuit voltage V_{OC}, the temperature difference ΔT $(T - T_{ref})$, the short circuit current $I_{sc,STC}$ and the open circuit voltage at STC $V_{OC,STC}$ have to be taken into account which gives

$$I_0 = \frac{I_{sc,STC} + K_i \cdot \Delta T}{e^{\frac{V_{OC,STC} + K_v \cdot \Delta T}{n \cdot N_s \cdot V_T}} - 1} \qquad (4)$$

Depending on the PV cell technology, the diode ideality factor n can be assumed as $n = 1.2$ (Habbati, 2014). The modified diode ideality factor $a = n \cdot N_s \cdot V_T$ varies with the number of cells connected in series N_s and the thermal voltage $V_T = \frac{k*T}{q}$. Taking into account the current I_{mpp} and voltage V_{mpp} at the maximum power point, the series resistance

$$R_s = \frac{V_{mpp}}{I_{mpp}} - \frac{n \cdot N_s \cdot V_T \cdot R_{sh}}{I_0 \cdot R_{sh} \cdot e^{\frac{V_{mpp} + I_{mpp} \cdot R_s}{n \cdot N_s \cdot V_T}} + n \cdot N_s \cdot V_T} \qquad (5)$$

and shunt resistance

$$R_{sh} = \frac{V_{mpp} + I_{mpp} \cdot R_s}{I_{ph} - I_{mpp} - I_0 \cdot (e^{\frac{V_{mpp} + I_{mpp} \cdot R_s}{n \cdot N_s \cdot V_T}}) - 1} \qquad (6)$$

can be calculated. Due to the very low series resistance and high shunt resistance, it is commonly assumed that $I_{ph} \approx I_{SC}$. With this approximation, the photovoltaic current I_{ph} can be calculated by $I_{ph} = \frac{R_{sh} + R_s}{R_{sh}} \cdot I_{sc}$. As the series resistance R_s, shunt resistance R_{sh} and photovoltaic current I_{ph} are mutually impacted by each other, their values are computed with the help of the Newton Raphson iteration method (Butenko et al., 2014). To investigate the shading effects for the overall plant, each module shall be taken into account with different irradiation and temperature values during simulation time. To build the $I - V$ curve of a whole PV array under shading conditions, several PV modules (denoted by number N) have to be connected either in series (i.e. N_{ser}) or in parallel (i.e. N_{par}) (Quaschning, 2016). In a series circuit of cells N_{ser}, the current $I_{ser} = I_{ser,1} = I_{ser,2} = \cdots = I_{ser,N_{ser}}$ is identical by all cells N_{ser}, the cell voltages $U(I)_{ser,unshaded} + N_{ser} \cdot U(I)_{ser,shaded}$ are summed up to the module voltage $U(I)_{ser}$. PV cells connected in parallel N_{par}, have all the same voltage $U_{par} = U_{par,1} = U_{par,2} = U_{par,3} = \cdots = U_{par,N_{par}}$. The cell currents of parallel cells are summed up to the total current $I_{par} = \sum_{n_{par}=1}^{N_{par}} I_{n_{par}}$.

To analyse the simulation time of a PV array under shading effects, a small PV power plant array with independent modules is modeled with the five-parameter single diode R_p-model. It is assumed that every module has its own bypass diode (Quaschning, 2016). The simulation in Matlab® takes about 0.25 s per module

and 0.88 s per PV array with 30 modules. A PV array with 30 modules takes ten times longer in Simulink™ then in Matlab® (see Figure 4). For a PV power plant consisting of 120 modules the simulation time is about 0.95 s in Matlab® and about 93 s in Simulink™. Simulating 120 modules in Matlab® is even 88 times faster than in Simulink™.

The Matlab® simulation time for a PV array with the size of the ground mounted PV power plant at the biogas plant Zellerfeld with a maximum 10,512 modules takes about 0.91 s.

4. Conclusions

The developed PV array modelling and simulation represents the first step towards the optimum interactive operation of the different renewable energy suppliers to avoid short-term, daily occurring grid overload in rural distribution grids. After analysing four different available PV models, the five-parameter single diode R_p-model is selected, due to its accuracy and computation time compared to other available modelling approaches. The developed PV models of the existing PV power plant are used as a model set, i.e. as input data for the control system at the biogas plant Zellerfeld. The model coded in Matlab® can provide an accurate electrical DC output for different types of PV modules checked against the nominal value of the manufacturer's data. The PV array simulation leads to a maximum time t_{cs} of 0.91 s under shading conditions, ensuring a sufficient over all reaction time for the control system.

Acknowledgements

References

Bär K., A. Saidi A., Zörner W., 2018a, Solar Irradiation Forecasting and Performance Simulation of Ground-Mounted Photovoltaic Power Plants, PV-Symposium, 644–672. (in German)

Bär K., A. Saidi A., Zörner W., 2018b, Report, FlexFuture- Integration of Biogas Plants in Rural Electricity Grids with a high Share of Fluctuating Power Generators, German Federal Ministry for Economic Affairs and Energy, Berlin, Germany. (in German)

Bundesministerium für Wirtschaft und Energie (BMWi) (Ed.), 2018, Renewable Energies in Numbers, 9-12. (in German).

Butenko S., Pardalos P., 2014, Numerical Methods and Optimization – An introduction, CRC Press, Abingdon, UK, 99-104.

Dotzauer M., Pfeiffer D., Lauer M., Pohl M., Mauky E.; Bär K., Sonnleitner M., Zörner W., Hudde J., Schwarz B., Faßauer B., Dahmen M., Rieke C., Herbert J., Thrän D., 2018, How to measure flexibility – performance indicators for demand driven power generation from biogas plants, Renewable Energy, 134, 135-146.

Habbati B., Ramdani Y., Moulay F., 2014, A detailed modeling of photovoltaic module using MATLAB, NRIAG J. Astron. Geophys., 3, 53–61.

Häring G., Sonnleitner M.; Bär K., Brown N., Zörner W., 2017, Demonstration of Controllable Electricity Production via Biogas Plants, Chem. Eng. Technol., 40, 298-305.

Heinrich Böll Foundation (Ed.), 2018, <energytransition.org/2018/11/renewables-in-germany/> accessed 03.04.2019.

Liu W., Ho W., Lee M., Hashim H., Lim J., Hoo P., Klemeš J., 2018, Optimising Thermal Power Plant with Generation Flexibility and Heat Rate Factor, Chemical Engineering Transactions, 70, 1981-1986.

Quaschning V., 2016, Understanding renewable energy systems, Earthscan Ltd, London, UK.

Stark M., Sonnleitner M., Zörner W., Greenough R., 2017, Approaches for Dispatchable Biomass Plants with Particular Focus on Steam Storage Devices, Chem. Eng. Technol., 40, 227–237.

Stark M.; Philipp M.; Saidi, A.; Trinkl, C.; Zörner, W.; Greenough R., 2018, Steam Accumulator Integration for Increasing Energy Utilisation of Solid Biomass-Fuelled CHP Plants in Industrial Applications, Chemical Engineering Transactions, 70, 2137-2143.

Sirch T., Bugliaro L., Zinner T., Möhrlein M., Vazquez-Navarro M., 2017, Cloud and DNI nowcasting with MSG/SEVIRI for the optimized operation of concentrating solar power plants. Atmospheric Measurement Techniques, 10(2), 409-429.

The MathWorks, Inc. (Ed.), 2019, <mathworks.com/> accessed 28.01.2019.

Valencia G., Obregón L., Cardenas Y., 2018, Comparison Analysis of an Energy Generation System Using Diesel, Natural Gas and Biogas as a Primal Fuel Resource, Chemical Engineering Transactions, 65, 301-306.